

Received May 21, 2020, accepted May 30, 2020, date of publication June 8, 2020, date of current version June 22, 2020.

Digital Object Identifier 10.1109/ACCESS.2020.3000638

Decision Boundary-Based Anomaly Detection Model Using Improved AnoGAN From ECG Data

DONG-HOON SHIN¹, ROY C. PARK², AND KYUNGYONG CHUNG³

¹Department of Computer Science, Kyonggi University, Suwon 16227, South Korea

²Department of Information Communication Software Engineering, Sangji University, Wonju 26339, South Korea

³Division of Computer Science and Engineering, Kyonggi University, Suwon 16227, South Korea

Corresponding author: Kyungyong Chung (dragonhci@gmail.com)

This work was supported by the Korea Agency for Infrastructure Technology Advancement (KAIA) grant funded by the Ministry of Land, Infrastructure and Transport (Grant 20CTAP-C157011-01).

ABSTRACT Arrhythmia detection through deep learning is mainly classified through supervised learning. Supervised learning progresses through the labeled data. However, in the medical field, it is challenging to collect ECG data of patients with arrhythmia than ECG data of healthy people, and thus data bias occurs. Therefore, if you use a supervised learning model, there are problems with lack of data and imbalance between labels that arise during learning. Accordingly, this study proposes the decision boundary-based Anomaly detection model using improved AnoGAN from ECG data. In this study, at the time of learning, the loss of the Generator does not reduce, but the loss of a Discriminator lowers. Even if the Generator and Discriminator were designed to have the same learning count, the learning competency of Generator was judged to be lowered. In repeated experiments, it was found that the best loss balance was achieved when the learning count of Discriminator was 1 and that of Generator was 4. Another problem is that the decision boundary of AnoGAN is subjective. Accordingly, the repeated experiments based on F-measure are conducted to determine a decision boundary. For performance evaluation, the accuracy of the model is evaluated on the basis of Epoch, and the goodness-of-fit of the model is evaluated on the basis of AUC and F-measure. According to the evaluation of F-measure, the model has the best performance when the decision boundary is 200. In terms of Epoch, the model has the highest accuracy when the Epoch is 10. In addition, the proposed model has better goodness-of-fit than AnoGAN.

INDEX TERMS Heart disease, arrhythmia, health care, deep learning, electrocardiogram, generative adversarial network, decision boundary, anomaly detection.

I. INTRODUCTION

According to the Cause-of-death statistics in the Republic of Korea reported by Statistics Korea, the three major causes of death are cancer, heart disease, and pneumonia. Their death rates account for 45% of the total ones [1]–[3]. Among these causes, heart disease has been the main death cause in the world over the last 15 years. The main cause of heart disease with a high death rate is arrhythmia [4], [5]. An arrhythmia is a problem with the irregular rate of one's heartbeat in the repeated contraction and relaxation of heart blood ejection. The main symptoms of arrhythmia include chest pain, heart palpitation, irregular heartbeat, dizziness,

asthenia, fatigue, and fainting, according to frequent pulse and slow pulse [6], [7]. In the early stages of onset, these symptoms arise intermittently. Most people ignore such symptoms and thus face complications [8]. Therefore, it is important to monitor a suspected arrhythmia patient's heart-beat continuously in his or her everyday life. For the detection of arrhythmia, an ECG signal is used. It represents the electrical activity of the heart and is used to detect and classify a cardiac arrhythmia. A cardiologist checks a patient's ECG waveform with the naked eye and determines whether the patient is diagnosed as an arrhythmia [9]. In fact, in order for a cardiologist to continue to monitor a suspected arrhythmia patient's ECG signals, it takes a lot of time and physical and human resources. For this reason, for auto arrhythmia detection, there has been active research on the algorithm

The associate editor coordinating the review of this manuscript and approving it for publication was Wei Wei¹.

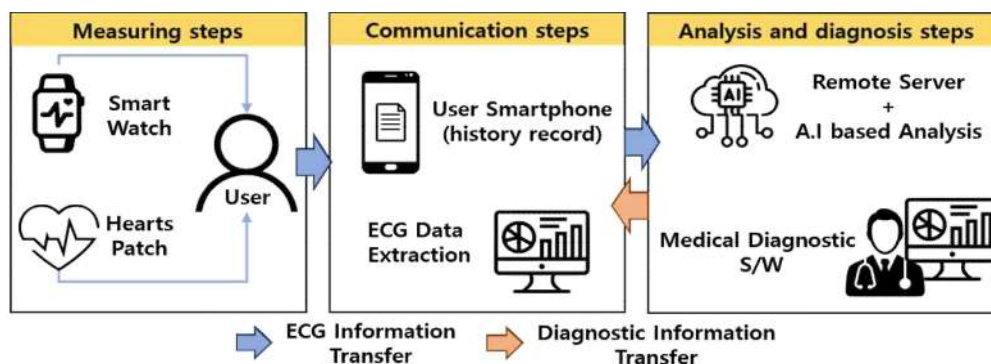


FIGURE 1. The structure of HUIINNO's heart disease care solution.

based on the morphological features of the QRS Complex or heartbeat [10]. However, it is hard to make an accurate diagnosis in such method, because there are a variety of heartbeat features: some arrhythmia has no morphological features of QRS Complex, and a heartbeat fluctuation can be high, though normal, depending on individuals [11]. Therefore, machine learning and deep learning-based arrhythmia detection have actively been researched these days. It is mostly subject to supervised learning-based detection or classification. However, in reality, arrhythmia data is significantly less than normal data without arrhythmia. Therefore, the data for supervised learning is insufficient and imbalanced. Accordingly, this study applies an anomaly detection method based on unsupervised learning. The methods based on unsupervised learning include Principle Component Analysis (PCA) [12], [13] One-Class Support Vector Machine (OCSVM) [14], [15] Autoencoders (AE) [16], [17] and Generative Adversarial Network (GAN) [18]. Principle Component Analysis (PCA) is capable of extracting data features and detecting an Anomaly going out of normal data. It has a limitation to the Anomaly detection of nonlinear data. One-Class Support Vector Machine (OCSVM) makes all data involved in one class to detect exceptional data going out of normal class. It has lower accuracy and high fluctuation of experimental results depending on the change of hyper-parameters. Autoencoders (AE) apply reconstruction and Anomaly detection to a nonlinear function. It is capable of detecting an Anomaly of data with a complex pattern. However, without appropriate normalization, it can cause overfitting and lower accuracy. Recently, Generative Adversarial Network (GAN) based Anomaly detection technique has been researched [19]. The representative Anomaly detection models based on GAN are Semi-Supervised Anomaly Detection via Adversarial Training (GANomaly) and Anomaly Detection Generative Adversarial Network (AnoGAN) [20], [21]. GANomaly additionally needs a test data set in the training process. It is semi-supervised learning, rather than unsupervised learning. Therefore, the model is not appropriate as the base model of this study. AnoGAN is unsupervised learning and learns with normal data. In the model, a decision boundary [22]

is subjective. Therefore, this study proposes the decision boundary based Anomaly detection model using the improved AnoGAN in ECG data. The proposed arrhythmia detection model is designed with the use of the GAN based AnoGAN that overcomes data imbalance and the problems of multiple models based on unsupervised learning. The problem that a decision boundary of AnoGAN is subjective is overcome in repeated experiments. In addition, to correct the imbalance of the loss generated in the learning process, this study improves AnoGAN.

This study is comprised of as follows: Chapter 2 explains the works related to deep learning-based arrhythmia detection techniques and AnoGAN based Anomaly detection models. Chapter 3 describes the proposed decision boundary based anomaly detection model using the improved AnoGAN. ECG data collection and pre-processing for the Anomaly detection, model design, training and validation, and anomaly score based decision boundary for classification are described. Chapter 4 describes the experimental method and results for evaluating the model performance. Chapter 5 provides the conclusion of this study.

II. RELATED WORK

A. DEEP LEARNING-BASED ARRHYTHMIA DIAGNOSIS TECHNOLOGY

HUIINNO, a Korean medical system manufacturer, developed the deep learning-based healthcare technology for heart diseases [23]. Fig. 1 show the heart disease care solution structure of HUIINNO. It measures ECG with time-series type and patch type wearable devices that make measurement on a regular basis and then sends the measured data to a cloud server that saves the data. The saved data is applied to ECG analysis through deep learning first and then is send to the medical staff for fast diagnosis and prescription. Based on the measured blood pressure and ECG information, relevant indexes are calculated and can be checked in an app.

Schlegl *et al.* [21] developed the Deep Convolutional Generative Adversarial Nets (DCGAN) based on Anomaly Detection Generative Adversarial Nets (AnoGAN) model for Anomaly detection. As an unsupervised learning model,

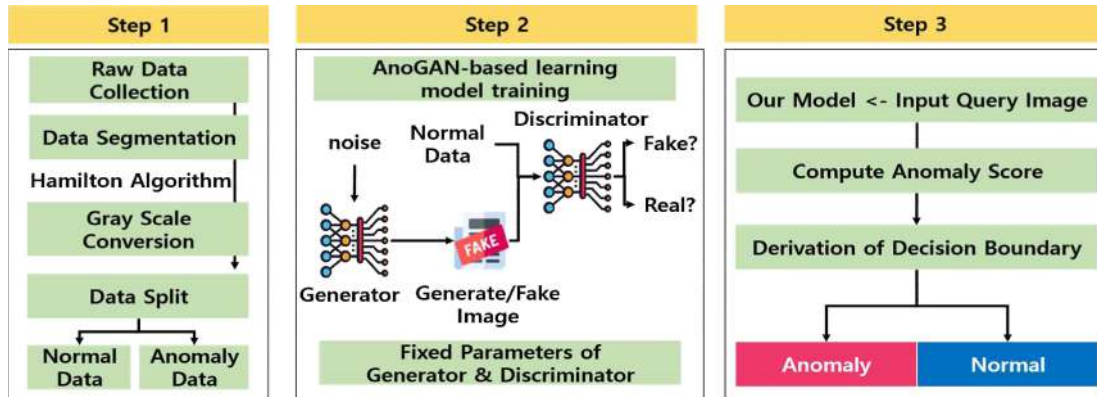


FIGURE 2. Process structure of anomaly detection model.

AnoGAN uses normal data for learning. By comparing with Query data, it is possible to detect an Anomaly. In the method, a decision boundary is subjective. Therefore, through repeated experiments, it is necessary to apply a decision boundary according to conditions.

To detect an Anomaly, Akcay *et al.* [20] proposed the Ganomaly (Semi-supervised Anomaly Detection) as a conditional generative adversarial network. In the proposed a discriminator network is trained with normal data for data distribution learning, and at the same time AE trains how to encode images effectively through data latent space. Ganomaly is a semi-supervised learning method. In its training process, the labelled data should be offered as training data. As for the labelled data, an expert needs to attach a note manually so that human resources are wasted.

For ECG classification, Alodia Yusuf and Hidayat [24] proposed the Euclidean distance based ECG classification method. The proposed method utilizes MFCC (Mel Frequency Cepstrum Coefficient) and Discrete Wavelet transformation and KNN in order to extract and classify features. The accuracy percentage of the proposed method is 84%, which is not high relatively.

In the research conducted by Huang *et al.* [25], Short-Time Fourier Transform (STFT) is applied for ECG Arrhythmia Classification so that signal data is converted into image data. 2D Convolution Neural Network (2D-CNN) is used for classification. Using a supervised learning model, the method is unable to predict the abnormal heartbeat, which is not within the category of the model.

B. ANOMALY DETECTION MODEL BASED ON AnoGAN

AnoGAN model learns with the use of normal data. Latent Space (z) represents a data of distribution probability. At the time of learning, the probability distribution of normal data approximates to Latent Space (z) through Generator (G). The data generated by G is learned in order for Discriminator (D) to discriminate that it is actual data. The model that completes learning does not update the parameters of G and D anymore. After the random sampling of Latent Space (z), the result is used as the input of the generator. Since the features of

normal data, the generator creates normal data. At this time, the created data is compared with Query data and Residual Loss is calculated. Query data including normal data and abnormal data. In equation (1), a value of Residual Loss can be calculated. In the equation, $LR(z_\gamma)$ means Residual Loss, $G(z_\gamma)$ is the generated data, and x represents Normal Image. If the generator learns sufficiently, the probability distribution of normal data approximates to Latent Space (z) and x and $G(z_\gamma)$ values are similar when x comes in G . Accordingly, the drawn value of Residual Loss is close to 0.

$$LR(z_\gamma) = \sum |x - G(z_\gamma)| \quad (1)$$

The discriminator determines if the data is True or False according to the probability distribution of the generated data. In this process, the value of Discrimination Loss is calculated. The Loss is used to appropriately map the data $G(z_\gamma)$ generated by z to the generator. The equation (2) shows Discrimination Loss. In the equation, $f(x)$ represents a probability distribution of Query data, and $f(G(z_\gamma))$ is a probability distribution of the generated data.

$$LD(z_\gamma) = \sum |f(x) - f(G(z_\gamma))| \quad (2)$$

Loss Function is used for Anomaly Score. A value of Total Loss is calculated to be used as the judgment basis of the anomaly. In equation (3), a value of Total Loss can be calculated. It is the addition of the value of Residual Loss and value of Discrimination Loss. At this time, λ is 0.1, $LR(z_\gamma)$ means Residual Loss, and $LD(z_\gamma)$ represents Discrimination Loss. The calculated value of Total Loss is used as Anomaly Score, which is the basis for determining if Query data as an input is normal or abnormal.

$$Total\ Loss = (1 - \lambda) * LR + \lambda * LD(z_\gamma) \quad (3)$$

III. DECISION BOUNDARY-BASED ANOMALY DETECTION MODEL USING IMPROVED AnoGAN FROM ECG DATA

This study proposes the decision boundary-based anomaly detection model using the improved AnoGAN in ECG data. The proposed method has a three-step process structure. Fig. 2 show the process structure of the anomaly

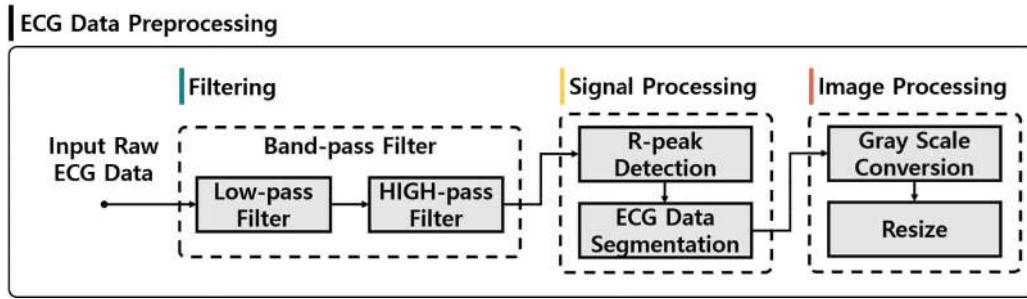


FIGURE 3. ECG data preprocessing.

detection model. As shown in the figure, the first step is ECG data collection and pre-processing. As data, MIT-BIH arrhythmia ECG data offered by Physionet are collected [26]. Pre-processing is performed to filter the data noises that arise in measurement. The model input is segmented to be designed by the ECG beat. The segmentation is made on the basis of the R-peak of ECG data. In terms of the beat-by-beat data, a 3D RGB channel is converted to a 2D grayscale channel in order to make it set to the model channel. Since the model used in this study utilizes a 2D-Convolution Layer, data is saved in an image format. The second step, the design, training and test of the improved AnoGAN based anomaly detection model for anomaly detection. In the step, the pre-processed Normal Image is used for learning. In the last step, for classification, a decision boundary is determined according to the change of anomaly score.

A. ARRHYTHMIA DATA COLLECTION AND PRE-PROCESSING FOR IMPROVED AnoGAN-BASED LEARNING

In this study, the MIT-BIH arrhythmia ECG data offered by Physionet is used for the learning of the proposed model [26]. The data is collected by Boston's Beth Israel Hospital. They consist of forty-eight 30-minute ECG data collected from twenty-five men aged 32-89 and twenty-two women aged 23-89 (a total of 47). Table 1 shows the data designed according to the characteristics of patients.

TABLE 1. Data designed by patient characteristics.

Record Series	No. of MIT-BIH Records
100	100, 101, 102, 103, 104, 105, 106, 107, 108, 109, 111, 112, 113, 114, 115, 116, 117, 118, 119, 121, 122, 123, 124
200	200, 201, 202, 203, 205, 207, 208, 209, 210, 212, 213, 214, 215, 217, 219, 220, 221, 222, 223, 228, 230, 231, 232, 233, 234

In table 1, twenty-three records (100 series) were randomly selected from 4,000 outpatients (40%) and inpatients (60%), and the other twenty-five records (200 series) are about the patients who have medically significant or

specific symptoms. The data are signal data consisting of ECG records. The records have two channels, most of which are limb lead type (MLII) and V1 type (exceptionally, V2, V4 or V5). The data evenly have 0.1~100Hz bandwidth filtering and 360Hz sampling speed. They are the arrhythmia data that include 15 classes of normal rhythms. In addition, the data information has notes written by an ECG specialist. The collected data are pre-processed to be used as the input data of the model. Fig. 3 shows ECG data preprocessing.

In Fig. 3, Raw ECG Data is the data actually measured with test subjects. If raw data are used as they are, it is hard to learn accurately with ECG DATA due to multiple noises that arise in measurement. Therefore, it is necessary to filter the ECG Data noises that occur in measurement. For filtering, Hamilton Algorithm is applied [27]. The algorithm makes use of Low Pass Filter (LPF) and High Pass Filter (HPF). LPF is used to remove the noises caused by the power interference in the ECG waveform. HPF is used to reduce the fluctuation of the ECG baseline. In order to design the filtered image by beat, R-peak is detected. Based on the detected R-peak, there are P-waves (followed by R-peak) and T-wave (following R-peak). For the beat design, segmentation is performed in the range between 0.3 seconds and 0.4 seconds on the basis of R-peak. The signal data designed by beat need to be converted into image data since the model utilizes 2D-Convolution Layer. The converted image is the real number with R, G and B in 3D. The model channel is equal to the image channel. If the number of model channels increases, the number of filters also rises and the time of operation becomes longer. Therefore, to shorten the operation time, the channel is lowered to the 2D channel through Gray Scale Conversion [28]. In addition, resizing is applied to match the input size (64×64) of the model with the size of the image. According to the recommendations of the Association for the Advancement of Medical Instrumentation (AAMI), 102, 104, 107 and 218 records have poor signal quality and thus need to be removed. Therefore, the pre-processed image data is reconstructed to be used for the learning and validation of the model [29]. Table 2 shows the Heartbeat Classes of MIT-BIH and the Heartbeat Classes of AAMI.

As shown in table 2, fifteen classes of MIT-BIH data are reconstructed in five classes according to the recommendations of AAMI. The reconstructed heartbeat classes of

TABLE 2. Heartbeat class of MIT-BIH and Heartbeat class of AAMI.

MIT-BIH Heartbeat Class	AAMI Heartbeat Class
Normal (N) Left Bundle Branch Block (L) Right Bundle Branch Block (R)	Normal (N)
Atrial Premature (A) Aberrated atrial Premature (a) Nodal (junctional) Premature (J) Supraventricular Premature (S) Atrial Escape (e) Nodal Escape (j)	Supraventricular(S)
Premature Ventricular Contraction (V) Ventricular Escape (E)	Ventricular(V)
Fusion of Ventricular and Normal (F)	Fusion(F)
Paced (/) Fusion of Paced and Normal (f) unclassified (Q)	Unknown(Q)

AAMI are Normal (N), Supraventricular (S), Ventricular (V), Fusion (F) and Unknown (Q). Learning occurs with the classified data in the model. In this study, the model learning is made only with normal data so that N Class is used. Data with other classes (S, V, F, and Q Class) than N Class are used as validation data. To check the correct classification of data, the model extracts and visualizes data features. To reduce the dimension of high-dimensional data, the linear dimensionality reduction using PCA (Principal Components Analysis) causes superposition. For this reason, t-distribution stochastic embedding (t-SNE) is applied [30], [31]. It is a nonlinear method for dimensionality reduction and visualization and well presents the feature of high-dimensional cluster relationships even in a low dimension. t-SNE consists of two steps. In the first step, features are extracted and a probability distribution is constructed according to the similarity of objects. In the second step, a probability distribution for objects in a low-dimensional space is defined, Kullback–Leibler divergence (KL divergence) between two distributions of object position is minimized [32]. Fig. 4 show the result of data visualization using the t-distribution stochastic embedding (t-SNE) based dimensionality reduction. In Fig. 4, ● represents Random noise, × Arrhythmia and ■ Normal. Unlike Random noise data, Arrhythmia and Normal data have a different category or arrhythmia and normal. Nevertheless, they are the same ECG data so that they are clustered in a proximity position. It means that they keep both global and local structures, which are the advantage of t-SNE. Keeping both global and local structure means not only that clustering is made appropriately, but that clustering occurs in a locationally close space if the data have similar features.

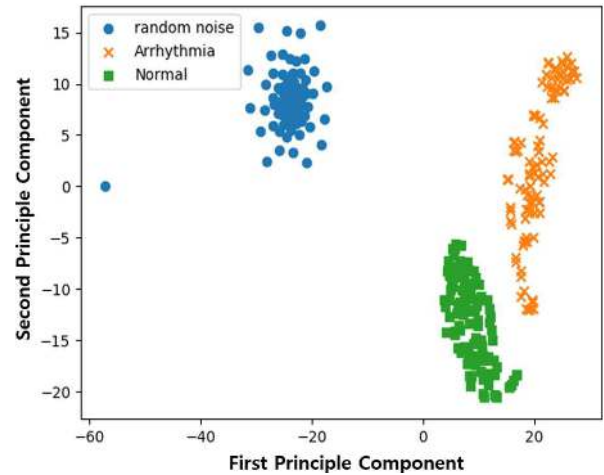


FIGURE 4. Result of data visualization using t-SNE based dimensionality reduction.

B. DESIGN OF IMPROVED AnoGAN-BASED ANOMALY DETECTION MODEL, TRAINING AND TESTING PHASE

In terms of modeling for prediction in analysis, it is possible to achieve Anomaly detection even with the use of a supervised learning model. In the health area, however, abnormal data with lesions are remarkably outnumbered by normal data without lesions, so that it is hard to collect data. For this reason, a supervised learning model has the problem of data imbalance and insufficiency. This study defines arrhythmia data as an Anomaly. Therefore, it utilizes AnoGNA, the GAN based unsupervised learning model using normal data only. Fig. 5 shows the structure of the Anomaly detection model. As shown in the figure, the model utilizes the GAN based AnoGAN, mainly consisting of Convolution Layer and Transposed Convolution Layer. Reaky Relu is used as an activation function and Dropout is applied to prevent overfitting at the time of learning. As input data, normal data are used and sizes 64×64 . The model detects an arrhythmia in the Anomaly detection network optimized from a target domain. The proposed Anomaly detection model performs learning in training phase and testing phase. Fig. 6 show the training phase and validation phase of the Anomaly detection model.

In the training phase of the figure, the normal images created by beat ($T(n)$) are used. In the phase, n represents the number of learning images. In the phase, Generator (G) and Discriminator (D) are learned, the probability distribution information of normal images approximates to Latent Space through z , the sampled low-dimensional noise. After the adversarial learning of G and D, which is the feature of GAN, an image is generated by G through Latent Space (z). And then, validation is made through the trained generator and Latent Space (z) with the distribution information of normal images. In the testing phase, the parameters of G and D are not updated. When Query Image (x) is given, the proposed model tries to find the optimal z , which is used to generate the image $G(z)$ similar to x . Based on the optimal z , an image

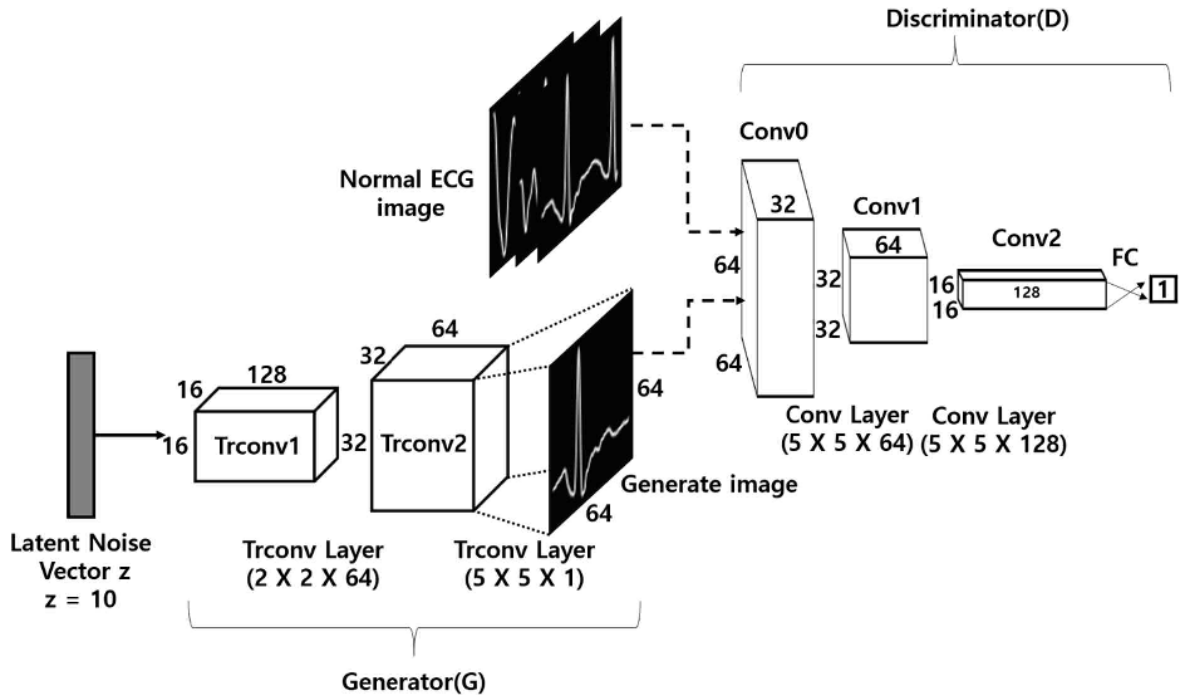


FIGURE 5. Structure of anomaly detection model.

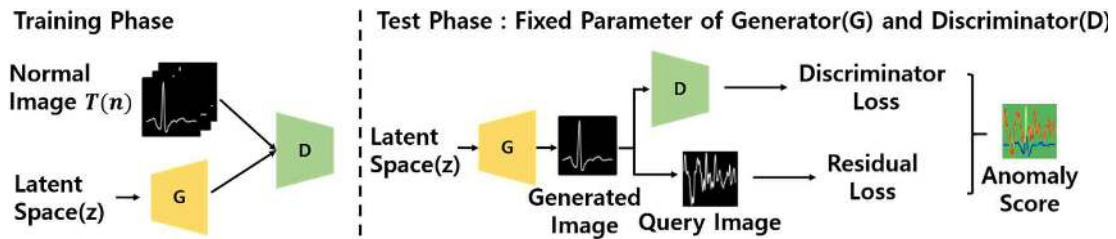


FIGURE 6. Training and testing phase in anomaly detection networks.

is generated and is compared with x . And then, a loss function is applied to calculate the value of the Anomaly Score. At this time, two-loss functions are defined. The first one is Residual Loss (R Loss), which is used to compare the difference between the image $G(z)$ generated by G and Query Image (x). The second one is Discriminator Loss (D Loss), which is used to determine that the probability distribution of the data D , the input image generated by $G(z)$, is True or False. Even if R Loss and D Loss process learning at the same time, R Loss fails to fall, but D Loss lowers. Unbalanced loss of generator and discriminator results in model inflexibility or inability to generate the correct form of data. For this reason, repeated experiments were conducted for learning stabilization. As a result, the best loss balance was achieved when the learning count of Generator was 4 and that of Discriminator was 1. Table 3 shows the function of making R Loss and D Loss balanced in terms of loss.

C. DECISION BOUNDARY CALCULATION THROUGH ANOMALY SCORE FOR CLASSIFICATION

For the classification into normal and arrhythmia data, a query image is used as an input of the model that finishes

learning and has a fixed weight. The input image is compared with the image created by the generator, so as to calculate a value of anomaly score. In AnoGAN model, a decision boundary is subjective. A decision boundary is a hyperplane in which a vector space is divided into two sets according to each class in the statistical classification with two classes. A classifier puts all points in one side of the decision boundary in one class and all points in the other side in the other class. This study defines a decision boundary with the use of anomaly score and then classifies data into normal and arrhythmia data. Fig. 7 show the subjective decision boundary defined with anomaly score. As shown in the figure, if a decision boundary is subjectively set to 350, arrhythmia data is classified into normal data. Therefore, it is necessary to validate the result of the image classified on the basis of the decision boundary. For validation, precision, recall and F-measure are applied [33], [34]. Precision means a ratio of actual True data to the True data determined by the model. Recall means a ratio of the True data predicted by the model to actual True data. Fig. 8 show the precision and recall according to changes of decision boundary in the Anomaly detection model.

TABLE 3. Loss balance function for learning stabilization.

```

Function: Loss Balance Function for Learning Stabilization.

Input: Train Data(x)
Output: G and D Loss
Train_Phase(x)
D ← Discriminator_model
G ← Generator_modela
for epoch(n)
    N ← Random Noise
    Real_Image ← Load data
    Generated_image ← G. predict(N)
    X ← Concatenate (Image, Generated_image)
    D.train(X)
    D.trainable ← False
    for range (3):
        G. train(N)
        D.trainable = True
return D, G
    
```

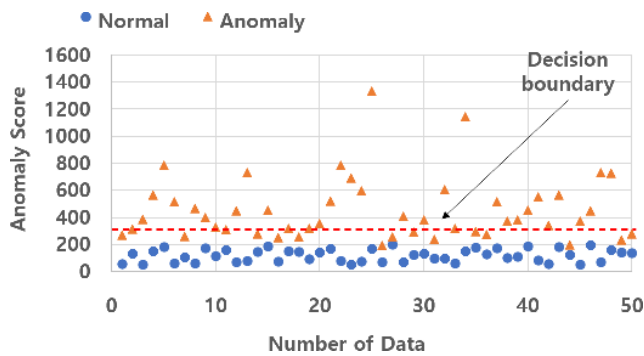


FIGURE 7. Subjective decision boundary determined by anomaly score.

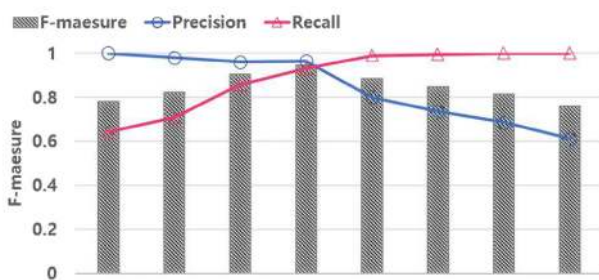


FIGURE 8. Precision and Recall according to change of the decision boundary.

In the figure, the crossing point of precision and recall curves occurs when a value of the anomaly score is 200. When the anomaly score is 200 and more, precision decreases but recall increases. With an increase in the decision boundary, the range for normal data decisions is widened and

recall increases. As a result, the data which should have been determined as arrhythmia data is judged to be normal, and thus precision falls. Therefore, when the decision boundary for normal/arrhythmia classification through repeated experiments is set to 200, precision and recall rates are the highest and the classification is the most accurate.

IV. RESULT AND PERFORMANCE EVALUATION

The experimental environment for implementing the proposed Anomaly detection model has such H/W and OS specifications: Window10 Pro, AMD Ryzen 5 1600 Six-Core Processor, NVIDIA GeForce GTX 1070 and RAM 16GB. As software, Tensorflow backend engine, and Deep learning library Keras are used. As the data for ECG experiments, the data with Five Classes-Normal (N), Supraventricular (S), Ventricular (V), Fusion (F) and Unknown (Q)-are reconstructed after the reclassification according to the recommendations AAMI [29]. The data are pre-processed, modeled and experimented in the way of the method proposed of this study. Table 4 shows the structure of learning data and validation data.

TABLE 4. Composition of train data and test data.

AAMI Class	Preprocess Data	Train Data	Test Data
Normal (N)	86717	85717	1000
Supraventricular(S)	3026	-	330
Ventricular(V)	7008	-	330
Fusion(F)	802	-	330
Unknown(Q)	15	-	15

In the modeling phase, normal data are used for learning so that normal (N) Class only is applied to construct learning data. In terms of N Class in table 4, 85,717 out of 86,717 data are used as learning data, and 1,000 as validation data. To set the ratio of validation data consisting of normal and arrhythmia data, this study uses 1,000 N Class data, 330 S Class data, 330 V Class data, 330 F Class data and 15 Q Class data. If the data ratio is not right and the number of normal data is large, the result of performance evaluation is likely to be biased.

A. PERFORMANCE EVALUATION

As the first item in the performance evaluation, the accuracy of the model is evaluated according to Epoch at the time of learning of the training model. Accuracy means a ratio of the total data used for testing to the accurately classified data [35], [36]. In the situation of class imbalance, it is necessary to prepare the scale that reflects a type of error in detail. Equation (4) show the mathematical expression of accuracy. In the formula, *TP* represents True Positive, *TN* is True Negative, *FP* is False Positive and *FN* is False Negative. An experiment is conducted in the condition that a

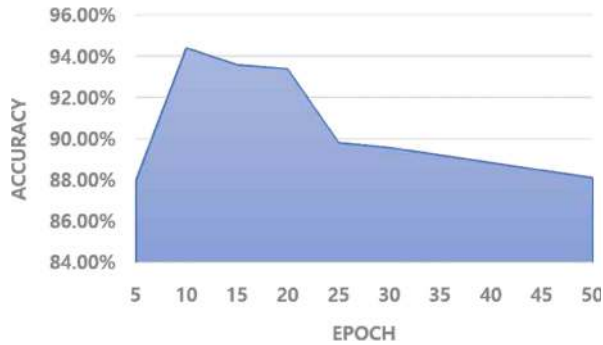


FIGURE 9. Results of model accuracy according to Epoch.

decision boundary is set to 200. Fig. 9 shows the result of the model accuracy, according to Epoch.

$$Accuracy (\%) = \frac{TP + TN}{TP + TN + FP + FN} \quad (4)$$

As a result of the performance evaluation, the proposed model has the most accuracy at 10 Epoch. It means that generalization performance lowers with more learning. Accordingly, with a rise in Epoch, the accuracy for Anomaly detection is evaluated to be low.

As the second item in the performance evaluation, the goodness-of-fit of the proposed model is evaluated. For the evaluation, the models using machine learning techniques (PCA, One Class Support Vector Machine (OCSVM) and Autoencoders (AE)) and the Anomaly detection models using AnoGAN model and the proposed improved AnoGAN are evaluated in terms of goodness-of-fit. The indexes used for the goodness-of-fit evaluation are Area Under a ROC Curve (AUC) and F-measure. AUC is the area of the base of the Receiver Operating Characteristic curve (ROC) [37]. AUC has a value range from 0 to 1. If it is closer to 1, sensitivity increases and specificity decreases. So, the performance is good. F-measure used as an index of accuracy appropriately reflects the trade-off of precision and recall [38], [39]. Table. 5 shows the result of the goodness-of-fit evaluation of the models according to AUC and F-measure.

TABLE 5. Model fit evaluation result according to AUC and F-measure.

Model	AUC	F-measure
K. Li et al. [15]	0.7917	0.7588
A. Gogna et. al. [17]	0.8944	0.8415
SAA Yusuf et. al. [24]	0.8312	0.8022
J. Huang et. al. [25]	0.9012	0.8633
S. Akcay et. al. [20]	0.9343	0.9042
T. Schlegl et. al. [21]	0.9272	0.8912
Our	0.9475	0.9143

As a result of the performance evaluation, the goodness-of-fit of PCA model is low since it has linear limitations. Autoencoders has relatively better performance than PCA, since the model can have non-linear weights on the basis of layers or can make dimensionality reduction. Although CNN and GANomaly have good performance, they need the labeled data in the learning and testing process. The improved model proposed in this study has higher AUC and F-measure values (0.023 and 0.0231 higher) than AnoGAN. The reason why the proposed model has good performance is that the decision boundary is objectively determined through objective modeling testing.

B. RESULT OF ANOMALY DETECTION FROM ECG DATA

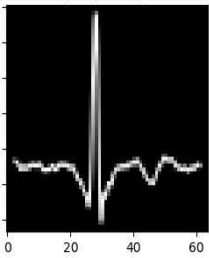
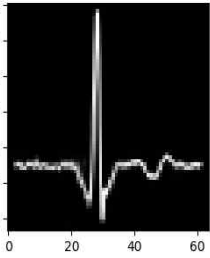
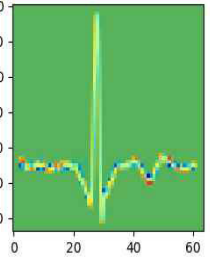
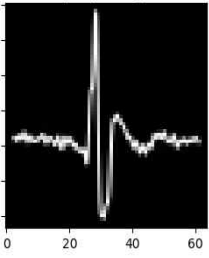
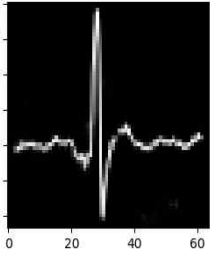
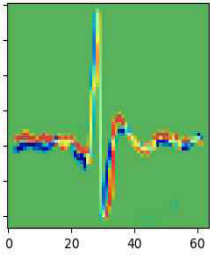
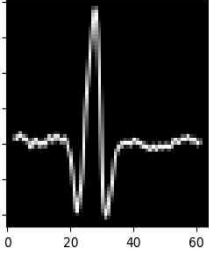
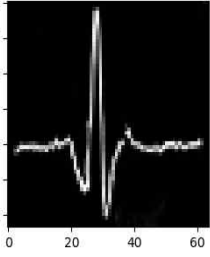
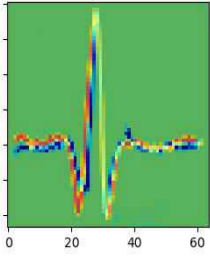
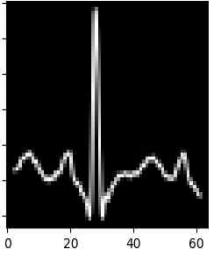
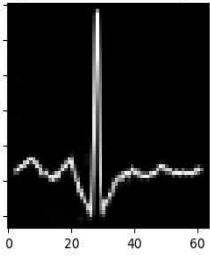
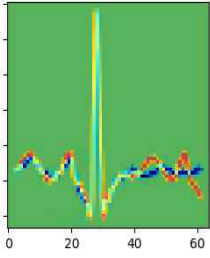
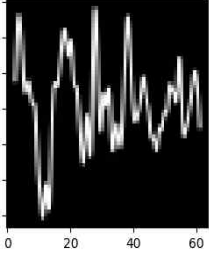
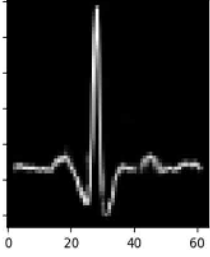
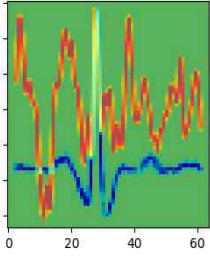
The detection result of the proposed Anomaly detection model from ECG data is presented. The difference between the generated image and the query image is compared. With the use of the anomaly score, a decision boundary is calculated. A value of the anomaly score is calculated in the way of adding the results of two-loss functions. Equation (5) is used to calculate the value of the anomaly score.

$$Anomaly\ score = (1 - \lambda) * R\ Loss + \lambda * D\ Loss \quad (5)$$

In the equation, R Loss means the Residual Loss of Generator and D Loss represents the Loss of Discriminator. Also, λ is set to 0.1, the value which shows the most efficient performance result in the tests of related work [21]. Experiments are conducted in the condition that a decision boundary is set to 200. Table 6 shows an Anomaly detection results of the comparison between the generated image and the input image of each AAMI Class.

As shown in Table 6 the Input Image (x) of each AAMI Class is used. The difference between the image G (z) generated by Latent Space (z) when the image (x) is used as an input by Generator (G) and x is visualized. The weight difference between G(z) and each pixel of x is calculated. It is mapped to the color map. The difference between the generated image and x is presented with a value of anomaly score (number). With the use of a decision boundary, the data is classified into normal and arrhythmia data. According to testing, when x of N is used as an input, Generator generates G(z) similar to the probability distribution of x. That is because the probability distribution of normal data approximates through Latent Space(z) at the time of the model learning. Accordingly, there is no visual difference in the comparison between x and G (z). G (z) generated after x of S, V, F or Q is used as an input is different from the probability distribution of x. That is because the probability distribution of normal data only is learned through z, but the probability distribution of arrhythmia data (S, V, F and Q) is not learned.

TABLE 6. Result of anomaly detection by AAMI class.

AAMI Class	Input Image(x)	Generated Image(G(z))	Anomaly Detection	Anomaly Score	Classification
N				170	Normal
S				454	Anomaly
V				497	Anomaly
F				351	Anomaly
Q				1401	Anomaly

V. CONCLUSIONS

This study proposed the decision boundary based Anomaly detection model using the improved AnoGAN in ECG data. In the medical area, normal data remarkably outnumbers abnormal data. To draw an effective result only with normal data, this study utilized GAN based AnoGAN as an unsupervised learning model. In AnoGAN, a decision boundary is subjective and has a loss imbalance. In this study, a decision

boundary was determined through experiments, and thus an objective value of decision boundary was calculated in terms of performance. In addition, with respect to loss imbalance, repeated experiments were conducted. As a result, it was found that the best loss imbalance occurred when the learning count of Generator was 4 and that of Discriminator was 1. In order to collect MIT-BIH arrhythmia data and design the input values by beat, this study detected R-Peak of ECG data

and conducted segmentation. For channel setting, Grayscale conversion was applied. For the input value of the training model and image size, 64×64 resizing was applied. Since the training model learned only with normal data, normal data were constructed. The test data for validation included normal and abnormal data. In the training process through the adversarial relationship between generator and discriminator, the generator created data to help the discriminator determine if the data is true, and the discriminator helped the model learn in the way of discrimination. The weight values of the generator and the discriminator of the trained model were fixed. The difference between the images generated when the query image was used as an input and query image was quantified, and thus a value of anomaly score was calculated. After repeated experiments with anomaly scores were conducted, a decision boundary was set to 200 through F-measure.

Based on the decision boundary, whether the data was normal or abnormal was determined. In terms of the model performance, the accuracy and goodness-of-fit of the model were evaluated according to Epoch. The model had the most accuracy at 10 Epoch. The proposed model based on the improved AnoGAN had better goodness-of-fit than the model based on AnoGAN. In other words, the AUC and F-measure of the proposed one were 0.023 and 0.0231 higher. Given the results, it is possible to detect an arrhythmia effectively only with normal data, and the proposed model, rather than the medical staff's continuous monitoring, makes it possible to manage an arrhythmia effectively. An unsupervised learning model like GAN can improve its performance depending on the amount of data.

The proposed model is expected to improve more its performance by applying prediction modeling for the analysis of angina and myocardial infarction data in the expansion of arrhythmia. In addition, the prediction modeling to be implemented through this study is expected to be greatly applicable to health decision-making.

VI. DISCUSSION

The proposed method detects an outlier with the use of normal ECG data only. In the healthcare area, normal data can be collected smoothly, whereas abnormal data such as lesions or nodes are difficult to be collected. In addition, it costs a lot to give a note to the information of lesion data. In this study, the distribution of normal data is learned on the basis of unsupervised learning, and query data are entered through the learned model. Query data include both normal and abnormal data. Since the model learns normal data only in the way of learning, it judges that abnormal input data is an outlier out of the normal data distribution.

A GAN model fails to generate data rightly or causes overfitting that makes the model inflexible, if Generator network and Discriminator model are out of balance. Accordingly, the two networks were balanced at the 1-to-4 ratio for right learning. The problem of AnoGAN is that a Decision Boundary is subjective. To solve the problem, this study calculated an objective decision boundary through repeated testing.

When the calculated decision boundary was 200, the best performance appeared. When the proposed model was compared with many different models, its AUC was 0.9475 and its F-measure was 0.9143 so that the model had the best performance. Although CNN and GANomaly have relatively good performance, they need the labelled data in the learning and testing process.

The previous studies using supervised learning had the restricted classification in the category of label. On contrary, this study detects the outlier of arrhythmia which is not in normal data. For the reason, it is possible to detect unlabeled arrhythmia.

REFERENCES

- [1] *Statistics Korea*. Accessed: Apr. 9, 2020. [Online]. Available: <http://kostat.go.kr/>
- [2] C.-W. Song, H. Jung, and K. Chung, "Development of a medical big-data mining process using topic modeling," *Cluster Comput.*, vol. 22, no. S1, pp. 1949–1958, Jan. 2019.
- [3] K. Chung and R. C. Park, "Cloud based U-healthcare network with QoS guarantee for mobile health service," *Cluster Comput.*, vol. 22, no. S1, pp. 2001–2015, Jan. 2019.
- [4] *World Health Organization (WHO)*. Accessed: Apr. 9, 2020. [Online]. Available: <https://www.who.int/>
- [5] M. Khoury, C. Jazra, and J. Abboud, "Cardiac arrhythmias," *Lebanese Med. J.*, vol. 67, no. 1, pp. 4–7, 2019.
- [6] *Korean Society of Cardiology (KSC)*. Accessed: Apr. 9, 2020. [Online]. Available: <https://circulation.or.kr/>
- [7] D. Schreiber, A. Sattar, D. Drigalla, and S. Higgins, "Ambulatory cardiac monitoring for discharged emergency department patients with possible cardiac arrhythmias," *Western J. Emergency Med.*, vol. 15, no. 2, pp. 194–198, 2014.
- [8] H. Yoo and K. Chung, "Heart rate variability based stress index service model using bio-sensor," *Cluster Comput.*, vol. 21, no. 1, pp. 1139–1149, Mar. 2018.
- [9] J. Pan and W. J. Tompkins, "A real-time QRS detection algorithm," *IEEE Trans. Biomed. Eng.*, vols. BME-32, no. 3, pp. 230–236, Mar. 1985.
- [10] P. E. Trahanias, "An approach to QRS complex detection using mathematical morphology," *IEEE Trans. Biomed. Eng.*, vol. 40, no. 2, pp. 201–205, Feb. 1993.
- [11] Y. Chen and H. Duan, "A QRS complex detection algorithm based on mathematical morphology and envelope," in *Proc. IEEE Eng. Med. Biol. 27th Annu. Conf.*, 2005, pp. 4654–4657.
- [12] R. J. Martis, U. R. Acharya, and L. C. Min, "ECG beat classification using PCA, LDA, ICA and discrete wavelet transform," *Biomed. Signal Process. Control*, vol. 8, no. 5, pp. 437–448, Sep. 2013.
- [13] V. Gupta and M. Mittal, "KNN and PCA classifier with autoregressive modelling during different ECG signal interpretation," *Procedia Comput. Sci.*, vol. 125, pp. 18–24, Jan. 2018.
- [14] S. M. Woo, H. J. Lee, B. J. Kang, and S. W. Ban, "ECG signal monitoring using one-class support vector machine," in *Proc. WSEAS*, Penang, Malaysia, Mar. 2010, pp. 23–25.
- [15] K. Li, N. Du, and A. Zhang, "Detecting ECG abnormalities via transductive transfer learning," in *Proc. ACM Conf. Bioinf., Comput. Biol. Biomed. BCB*, 2012, pp. 210–217.
- [16] J. An and S. Cho, "Variational autoencoder based anomaly detection using reconstruction probability," *Special Lect. IE*, vol. 2, no. 1, pp. 1–18, 2015.
- [17] A. Gogna, A. Majumdar, and R. Ward, "Semi-supervised stacked label consistent autoencoder for reconstruction and analysis of biomedical signals," *IEEE Trans. Biomed. Eng.*, vol. 64, no. 9, pp. 2196–2205, Sep. 2017.
- [18] A. Creswell, T. White, V. Dumoulin, K. Arulkumaran, B. Sengupta, and A. A. Bharath, "Generative adversarial networks: An overview," *IEEE Signal Process.*, vol. 35, no. 1, pp. 53–65, Jan. 2017.
- [19] R. Chalapathy and S. Chawla, "Deep learning for anomaly detection: A survey," 2019, *arXiv:1901.03407*. [Online]. Available: <http://arxiv.org/abs/1901.03407>
- [20] S. Akcay, A. Atapour-Abarghouei, and T. P. Breckon, "GANomaly: Semi-supervised anomaly detection via adversarial training," 2018, *arXiv:1805.06725*. [Online]. Available: <http://arxiv.org/abs/1805.06725>

- [21] T. Schlegl, P. Seeböck, S. M. Waldstein, U. Schmidt-Erfurth, and G. Langs, "Unsupervised anomaly detection with generative adversarial networks to guide marker discovery," in *Information Processing in Medical Imaging*. Berlin, Germany: Springer, Jun. 2017, pp. 146–157.
- [22] H. Watanabe, R. Togo, T. Ogawa, and M. Haseyama, "Bone metastatic tumor detection based on AnoGAN using CT images," in *Proc. IEEE 1st Global Conf. Life Sci. Technol. (LifeTech)*, Osaka, Japan, Mar. 2019, pp. 235–236.
- [23] *Huinno*. Accessed: Apr. 9, 2020. [Online]. Available: <https://www.huinno.com/>
- [24] S. A. Alodia Yusuf and R. Hidayat, "MFCC feature extraction and KNN classification in ECG signals," in *Proc. 6th Int. Conf. Inf. Technol., Comput. Electr. Eng. (ICITACEE)*, Sep. 2019, pp. 1–5.
- [25] J. Huang, B. Chen, B. Yao, and W. He, "ECG arrhythmia classification using STFT-based spectrogram and convolutional neural network," *IEEE Access*, vol. 7, pp. 92871–92880, 2019.
- [26] G. B. Moody and R. G. Mark, "The impact of the MIT-BIH arrhythmia database," *IEEE Eng. Med. Biol. Mag.*, vol. 20, no. 3, pp. 45–50, Jun. 2001.
- [27] L. Sathyapriya, L. Murali, and T. Manigandan, "Analysis and detection R-peak detection using modified pan-tompkins algorithm," in *Proc. IEEE Int. Conf. Adv. Commun., Control Comput. Technol.*, May 2014, pp. 483–487.
- [28] C. Saravanan, "Color image to grayscale image conversion," in *Proc. 2nd Int. Conf. Comput. Eng. Appl.*, Mar. 2010, pp. 196–199.
- [29] *Testing and Reporting Performance Results of Cardiac Rhythm and ST Segment Measurement Algorithms*, Arlington, VA, USA: Association for the Advancement of Medical Instrumentation, 1998.
- [30] L. van der Maaten and G. Hinton, "Visualizing data using t-SNE," *J. Mach. Learn. Res.*, vol. 9, pp. 2579–2605, Nov. 2008.
- [31] L. van der Maaten, "Accelerating t-SNE using tree-based algorithms," *J. Mach. Learn. Res.*, vol. 15, no. 1, pp. 3221–3245, Oct. 2014.
- [32] T. van Erven and P. Harremoës, "Rényi divergence and Kullback-leibler divergence," *IEEE Trans. Inf. Theory*, vol. 60, no. 7, pp. 3797–3820, Jul. 2014.
- [33] J.-W. Baek and K. Chung, "Context deep neural network model for predicting depression risk using multiple regression," *IEEE Access*, vol. 8, pp. 18171–18181, 2020.
- [34] K. Chung and J. Kim, "Activity-based nutrition management model for healthcare using similar group analysis," *Technol. Health Care*, vol. 27, no. 5, pp. 473–485, Sep. 2019.
- [35] H. Jung and K. Chung, "Sequential pattern profiling based bio-detection for smart health service," *Cluster Comput.*, vol. 18, no. 1, pp. 209–219, Mar. 2015.
- [36] J. W. Baek, J. C. Kim, J. Chun, and K. Chung, "Hybrid clustering based health decision-making for improving dietary habits," *Technol. Health Care*, vol. 27, no. 5, pp. 473–485, Sep. 2019.
- [37] K. Hajian-Tilaki, "Receiver operating characteristic (ROC) curve analysis for medical diagnostic test evaluation," *Caspian J. Internal Med.*, vol. 4, no. 2, pp. 627–635, 2013.
- [38] M. Buckland and F. Gey, "The relationship between recall and precision," *J. Amer. Soc. for Inf. Sci.*, vol. 45, no. 1, pp. 12–19, Jan. 1994.
- [39] M. Gordon and M. Kochen, "Recall-precision trade-off: A derivation," *J. Amer. Soc. Inf. Sci.*, vol. 40, no. 3, pp. 145–151, May 1989.



DONG-HOON SHIN received the B.S. degree from the Department of Computer Engineering, Dongseo University, South Korea, in 2019. He is currently pursuing the master's degree with the Department of Computer Science, Kyonggi University, Suwon, South Korea. He has been a Researcher with the Data Mining Laboratory, Kyonggi University. His research interests include data mining, artificial intelligent, healthcare, biomedical and health informatics, knowledge systems, VR/AR, and deep learning.



ROY C. PARK received the B.S. degree from the Department of Industry Engineering, Sangji University, Wonju, South Korea, and the M.S. and Ph.D. degrees from the Department of Computer Information Engineering, Sangji University, in 2010 and 2015, respectively. From 2015 to 2018, he was a Professor with the Division of Computing Engineering, Dongseo University, South Korea. Since 2019, he has been a Professor with the Department of Information Communication Software Engineering, Sangji University. His research interests include WLAN systems, heterogeneous networks, ubiquitous network service, human-inspired artificial intelligent and computing, health informatics, knowledge systems, peer-to-peer, and cloud networks.



KYUNGYONG CHUNG received the B.S., M.S., and Ph.D. degrees from the Department of Computer Information Engineering, Inha University, South Korea, in 2000, 2002, and 2005, respectively. He has worked for the Software Technology Leading Department, Korea IT Industry Promotion Agency (KIPA). From 2006 to 2016, he was a Professor with the School of Computer Information Engineering, Sangji University, South Korea. Since 2017, he has been a Professor with the Division of Computer Science and Engineering, Kyonggi University, Suwon, South Korea. His research interests include data mining, artificial intelligent, healthcare, biomedical and health informatics, knowledge systems, HCI, and recommendation systems.

• • •